IEEE Transactions on Industry Applications, Vol. 37, No. 5, Sept./Oct. 2001, pp. 1299-1307.

An Efficient Braking Method for Controlled AC Drives with a Diode Rectifier Front End

J. Jiang, *Member*, and J. Holtz, *Fellow, IEEE*
University of Wuppertal
42097 Wuppertal – Germany

Abstract — **Standard PWM inverter fed induction motor drives employ a diode rectifier bridge to supply ac power from the utility to the dc link. Although a diode rectifier is the most cost-effective solution, it does not permit reversing the power flow. This prohibits operating the machine in the regenerative braking mode for active deceleration. An innovative control method substitutes conventional hardware, such as an active front-end rectifier or a chopper controlled braking resistor in the dc link circuit, by additional software that is implemented in a standard microprocessor control. The control algorithm maximizes the power losses in the machine and in the inverter. It enables regenerative braking operation of the induction motor at high torque. The algorithm conserves the high dynamic performance of a vector controlled drive system.**

1. INTRODUCTION

Induction machines fed from a pulsewidth modulated power converter have become the preferred solution for adjustable speed drive applications [1]. The standard configuration of such drive system is shown in Fig. 1. The electrical energy is usually supplied from the 3-phase utility. The line voltage is rectified and then used to maintain the voltage u_d of a dc link capacitor C at a fixed level, which is determined by the line voltage amplitude. The capacitor voltage is u_{dR} at nominal operation.

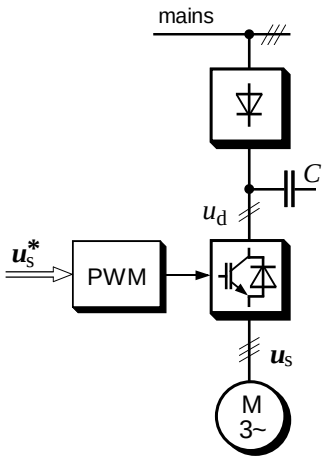

Fig. 1: PWM inverter with diode rectifier front end

It is preferred to use a diode bridge as front end rectifier because of its low cost. It is a disadvantage that a diode bridge is not capable of regenerating power to the ac supply. Since an ac drive is able to operate in all four quadrants of the torque-speed plane, power will be regenerated into the dc link when the induction machine works in the generating mode. The reversal of power flow will consequently raise the dc link voltage above its normal operation value, and steps must be taken to absorb the regenerated power to prevent a dangerous increase of the dc link voltage.

Many ac drives are designed such that power regeneration is inhibited. Braking operation is then impossible, which limits the range of application. Alternatively, an electronically controlled resistor (not shown in Fig. 1) in parallel to the dc link capacitor can be used to absorb the regenerated energy [2]. This requires additional power electronic components and electronic control circuits, and thus increases the cost and complexity of the ac drive and reduces its reliability. Even more expensive is the use of an active rectifier front end which is employed only in special cases.

To avoid using a switched resistor or any other energy absorbing hardware, and thus reduce the cost, it has been proposed to dissipate the regenerated energy in the ac motor and to some extent in the feeding inverter. To facilitate an understanding of the principles of such methods, it will be subse-

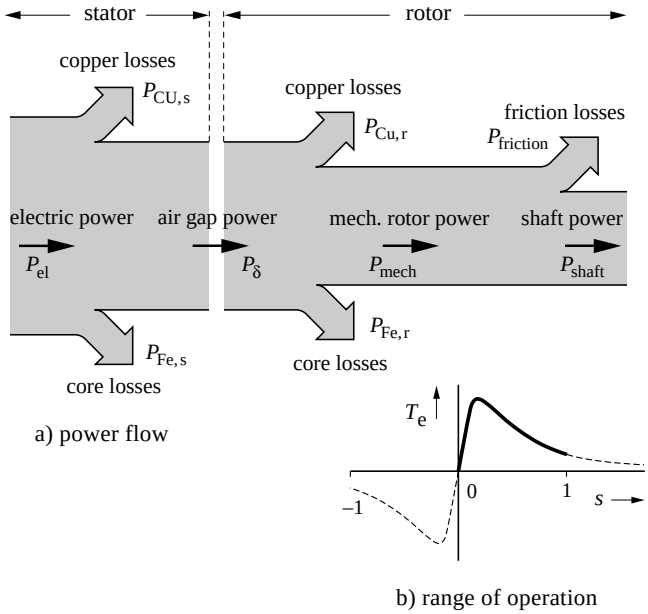

Fig. 2: Motoring mode

quently discussed which kinds of losses exist in an induction motor and how these losses can be used to dissipate the regenerated energy.

2. Induction Motor Losses

The different sources of losses in the induction machine are illustrated in the power flow diagram Fig. 2. Motoring operation is considered first where the slip s ranges between 0 and 1 ($0 < s < 1$). The electrical input power of a 3-phase machine is given by

$$P_{el} = 3V_s I_s \cos\varphi \qquad (1)$$

where V_s is the phase voltage,
I_s is the phase current, and
$\cos\varphi$ is the displacement factor.

Machine losses occur both in the stator and in the rotor. The losses in the stator are:

1. Copper losses $P_{Cu,s}$ in the stator windings, which are proportional to the square of the stator current I_s

$$P_{Cu,s} = 3I_s^2 R_s, \qquad (2)$$

where R_s is the ohmic resistance of the phase windings.

2. Stator core losses $P_{Fe,s}$ include hysteresis and eddy current losses. They depend on the magnitude of the stator flux and the stator frequency f_s.

The power that remains after deducting $P_{Cu,s}$ and $P_{Fe,s}$ from P_{el} is the air gap power P_δ. The air gap power is transferred from the stator to the rotor through the air gap. In the rotor, a portion of the air gap power is dissipated as losses in the rotor. These losses are:

3. The copper losses in the rotor windings, which are proportional to the square of the rotor current I_s:

$$P_{Cu,r} = 3I_r^2 R_r, \qquad (3)$$

where R_r is the ohmic resistance of the equivalent phase windings of the rotor.

4. The rotor core losses $P_{Fe,r}$ which include hysteresis and eddy current losses and depend on the magnitude of the rotor flux and on the rotor frequency. At normal operating condition, the frequency f_r of the rotor currents is low and then these losses can be neglected.

The remaining power is converted into mechanical power. A portion of it covers the windage and friction losses, which losses depend on the rotor speed. The rest is finally the mechanical power P_{shaft} at the motor shaft, which is the useful output power of the machine. It is assumed here for simplicity that the mechanical inertia of the rotor is contained in the mechanically coupled load. The rotor is then considered as having zero inertia and the inertial torque component is contained in the shaft power.

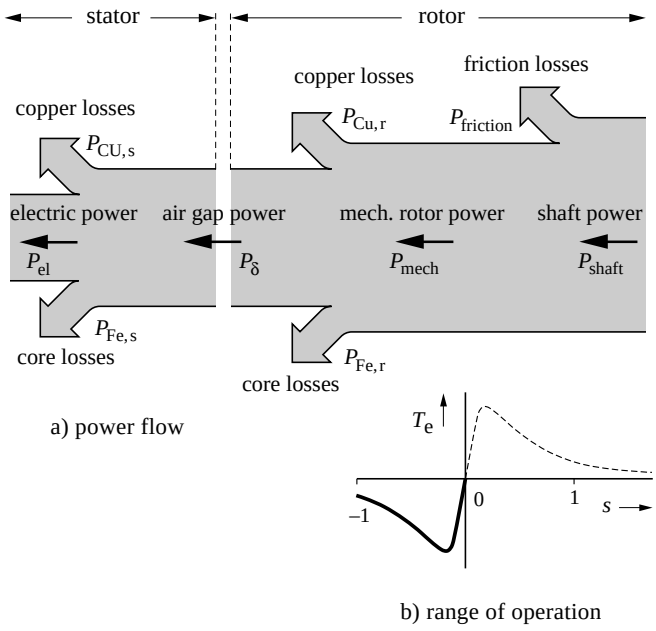

Fig. 3: Generating mode

Taking the example of a 10-kW induction motor, the losses typically subdivide as follows:

stator copper losses	$P_{Cu,s} = 0.6\ P_{total}$
stator core losses	$P_{Fe,s} = 0.25\ P_{total}$
rotor copper losses	$P_{Cu,r} = 0.15\ P_{total}$

Table I

P_{total} are the total losses of the motor. Friction and windage losses are not taken into consideration even though they improve the performance during braking. The rotor core losses can be neglected at nominal operation since the rotor frequency equals the slip frequency and hence is very low.

It can be seen from the example that most of the motor losses occur in the stator. The rotor losses are small in comparison with the stator copper and stator core losses.

To reduce the shaft speed of an induction motor by braking, a braking torque is required to counteract an active torque generated by the mechanically coupled load and by the inertia of the drive train. The shaft power P_{shaft} is negative during braking. Depending on the sign of the slip s, there are two modes of operation.

The generating mode is characterized by the power flow schematic shown in Fig. 3. The slip is negative ($s < 0$), which means that the stator field and the rotor rotate in the same direction, and the stator field rotates slower than the rotor. As a result, the air gap power P_δ is negative. Unless the motor operates at very low speed, the air gap power is larger than the stator losses such that the electrical power P_{el} of the stator winding is negative. In this case, all motor losses, and the electrical power P_{el} as well, are supplied by the negative shaft power P_{shaft}.

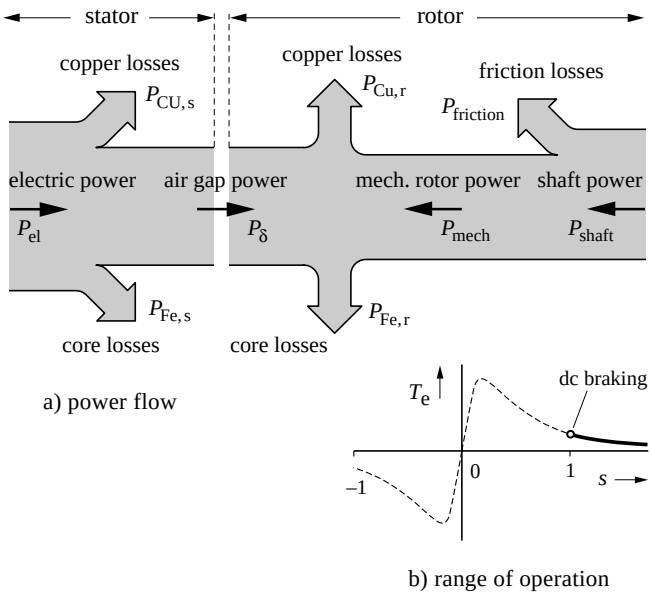

Fig. 4: Plugging mode

The second operating mode which can be used for braking is the plugging mode: The slip is positive, $s > 1$. The stator field and the rotor rotate in different directions. Fig. 4 illustrates the power flow in this situation. The stator losses are exclusively supplied by the inverter while the rotor losses are supplied partly by the inverter and partly by the shaft power.

In case of $s = 1$ the stator frequency is zero. This condition characterizes the well known dc braking method which will be discussed in the following Section.

3. Conventional Braking Schemes

3.1 Regenerative braking

The only efficient braking scheme that presently exists is regenerative braking. The braking torque produces negative shaft power which is regenerated by the motor and fed through the inverter into the dc link circuit. It is then dumped into an electronically controlled braking resistor or regenerated into the utility by a line-controlled power converter, or by an active front end rectifier. All methods require controlled power conversion systems, which entails heavy cost penalties. Hence these methods are not further considered.

3.2 DC braking

In the absence of controllable power circuits that absorb the regenerated power from the dc link circuit, the method of dc braking can be used. The machine is then operated at zero stator frequency, although its mechanical angular velocity is high. The operating point of the machine at dc braking is marked in Fig. 4(b).

The induced rotor currents produce resistive losses in the rotor bars and the energy thus absorbed serves as the braking energy of the machine. Since the stator field does not rotate at dc braking, the rotor induced voltage is zero and the machine does not generate electrical power which would accumulate in the dc link capacitor. Hence the scheme works well with a passive diode rectifier front end.

The operation of dc braking can be implemented by an appropriate control scheme. To initiate dc braking, the stator flux is first controlled to near zero, and then a dc voltage is generated by the inverter to establish maximum dc current flow in the stator windings. Although the stator current assumes its maximum value, the resulting braking power is very small. The stator flux does not rotate and hence the air gap power is zero. The stator copper losses are maximum, but they do not contribute to the braking power as they are supplied by the inverter. The stator core losses are zero since the stator frequency is zero. The rotor core losses are negligible since most of the stator flux linkage develops as leakage flux and the rotor flux is very small. Only the energy dissipated in the rotor resistances is supplied by the shaft power, and hence the braking power is low.

Referring to typical values of machine losses as shown in Table 1, the rotor copper losses and hence the braking power amount to only 15% of the total machine losses. This means that the capability of the motor to dissipate the braking power is badly exploited. The lower curve in Fig. 5 shows that only a braking torque of less than 10% of the nominal torque can be achieved over a wide speed range.

Apart from the poor ability to develop a braking torque, the method of dc braking also exhibits a poor dynamic performance. The reason is that the machine flux can not be abruptly changed. Before the braking torque is initially developed, a time delay which corresponds the rotor time constant τ_r elapses during which the flux decays to the required small amplitude. When returning to motoring operation, it takes the same time delay until the original flux is reestablished.

The low braking torque and the poor dynamic performance are the reasons why dc braking is rarely employed for ac drives, although the implementation would just require adding some software code to the microprocessor algorithm.

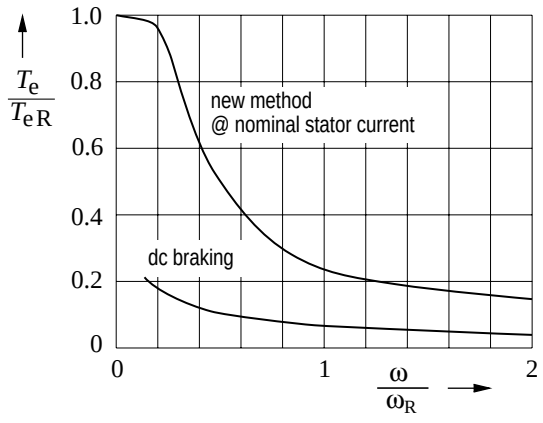

Fig. 5: Maximum braking torque versus speed for two different braking methods

3.3 Braking with added harmonic machine currents

This approach aims at increasing the machine losses by injected harmonic currents [2]. Undesired side effects are the radiation of acoustic noise and high torque ripple which make this method little attractive.

3.4 Braking in the field oriented mode

A shaft power of negative value, $P_{shaft} < 0$, is called braking power in the following. Considering the mechanical speed ω constant, the developed braking torque is proportional to the shaft power P_{shaft}. To make the braking torque as high as possible, maximum braking power must be obtained. Since there is no energy consumed in the dc link, the braking power is mostly absorbed in the motor, and to some extent in the inverter.

High dynamic performance is achieved using the principle of field oriented control, also known as vector control [3]. Here, the stator current vector is processed in a field oriented coordinate system. It is decomposed into its orthogonal components, $\boldsymbol{i}_s = i_d + j i_q$, of which the quadrature current component i_q controls the torque, and in-phase current component i_d controls the rotor field.

Braking is performed when the speed reference ω^* is lower than the measured motor speed ω. The motor operates in the generating mode, but its torque is limited such that the dc link voltage does not increase. The generated power just covers the system losses. The motor field, and consequently the stator core losses, are maintained at nominal values. Since the power regenerated into the dc link is zero, the airgap power equals the stator losses. The *q*-current and the rotor currents are then very small. Their contributions to the copper losses can be neglected. It is only the *d*-current that produces copper losses in the stator. The *d*-current is typically 30% of the nominal stator current. Since the copper losses are proportional to the square of the current, the losses at field oriented braking, expressed by the rated losses from Table I, are

$$\begin{aligned} P_{FO} &= P_{Fe,s} + 0.3^2 P_{Cu,s} = (0.25 + 0.05) P_{total} \\ &= 0.30\, P_{total} \end{aligned} \tag{4}$$

This means that the motor dissipates only 30% of its nominal losses at field oriented braking.

4. Maximum System Loss Control

4.1 Description of the method

An efficient braking scheme must aim at maximizing the power dissipation in the motor, which in turn maximizes the braking torque.

To maximize the stator and rotor copper losses, the stator currents and the rotor currents must be maximum, even when operating at reduced torque. The maximum stator core losses occur when the stator flux is maximum and the stator frequency is high. Moreover, all losses must be supplied by the shaft power, not by the inverter. To be generally applicable, high dynamic torque control must be possible. The method should be workable in speed control systems with speed sensor and without speed sensor.

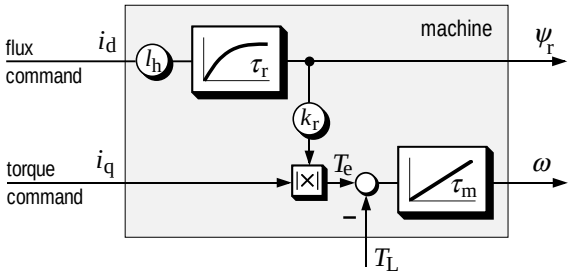

Fig. 6: Dynamic model of the induction motor at field orientation

The control scheme presented in this paper satisfies the aforementioned requirements. To ensure high dynamic performance, the scheme is devised as an extension of the field oriented control approach. It improves this method such that efficient braking is enabled without accumulating the regenerated power in the dc link.

The new method [4] is explained in the following. At field oriented control, the electromagnetic torque

$$T_e = k_r \psi_r i_q \tag{5}$$

is proportional to the rotor flux linkage ψ_r and the *q*-axis current i_q. The coefficient $k_r = l_h / l_r$ is the coupling factor of the rotor, l_h is the mutual inductance between stator and rotor windings and l_r is the inductance of the rotor winding. The rotor flux linkage ψ_r is defined by the differential equation

$$\tau_r \frac{d\psi_r}{dt} + \psi_r = l_h \boldsymbol{i}_d \tag{6}$$

where $\tau_r = l_r / r_r$ is the normalized rotor time constant. Equations (5) and (6) are visualized in the signal flow graph [3] shown in Fig. 6.

To maximize the stator copper losses, the rms value of the stator current

$$i_{rms} = \sqrt{\frac{1}{T} \int_T \left(i_d^2 + i_q^2 \right) dt} \tag{7}$$

must be maximum. Assuming in a first step that the inverter has no overload capability, the limiting quantity is the maximum inverter current. It is assumed that this current equals the nominal stator current i_{sR} of the machine, $i_{rms} = i_{sR}$. Unfortunately, operation at nominal stator current is not possible at braking, since there are constraints on both current components, i_d and i_q, on the right-hand side of (7):

1. The *d*-current i_d is limited to about 30% of the nominal stator current in the base speed range, and to lower values at field weakening. A higher *d*-current would overmagnetize the machine, giving rise to excessive magnetic noise in the base speed range, and to prohibitive overvoltages at field weakening.
2. Since the *q*-current controls the torque according to (5),

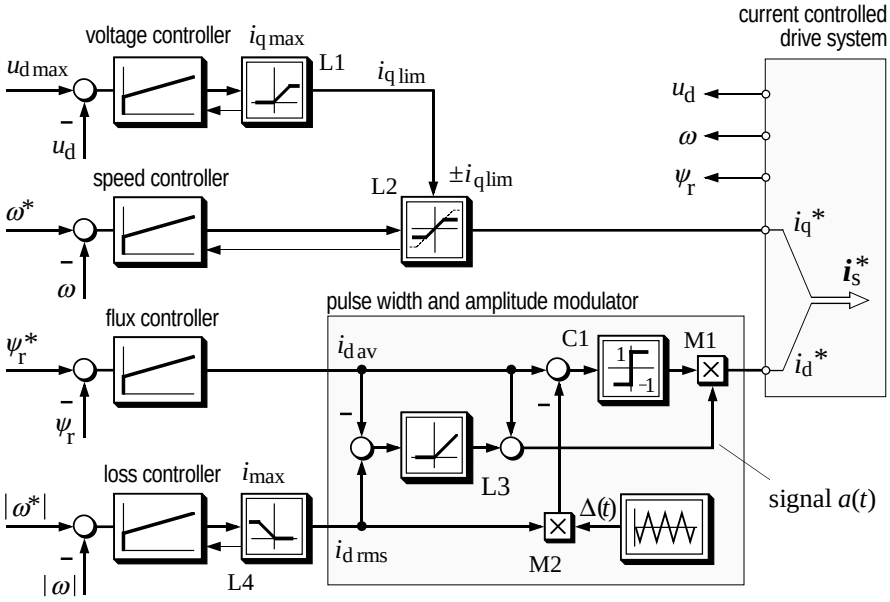

Fig. 7: Signal flow graph of the braking control scheme;
value of signal a: $a = i_{d\,av}$ at motoring, $a = i_{d\,rms}$ at braking

its magnitude is limited to fairly low values in the braking mode. The reason is that the braking power must not exceed the system losses which are low as compared with the power rating of the machine.

These constraints are circumvented by the new control method, according to which a high-frequency square-wave current is superimposed on the *d*-current i_d. Although the required average value of i_d is then still maintained, its rms value is increased. Rapid changes of the magneto-motoric force (mmf) are then commanded in the stator. The high-frequency changes of the stator mmf induce similar changes in the rotor mmf. As a consequence, both the rms values of the stator current and of the rotor current increase, thus increasing the copper losses in the stator and in the rotor. Also the iron losses increase, which is predominantly due to the high-frequency leakage fields in the teeth.

The additional losses are controlled to a desired magnitude by varying the magnitude of the injected high-frequency currents.

The method has the following advantages:

1. The total machine losses at braking can be made higher than the total nominal machine losses P_{total}.
2. The losses can be further increased if the inverter is capable of delivering more than the rated machine current. Such overload capability is frequently incorporated in the inverter. It serves for short-time acceleration at higher than nominal torque.

   Operation at overcurrent is advantageous since the copper losses increase with the square of the current.
3. Also the losses in the inverter are supplied by the machine and hence contribute to the braking power.

The injected high-frequency components do not have adverse effects on the machine performance. Fig. 6 shows that the large rotor time τ_r constant attenuates the high-frequency i_d-current components and hence almost eliminates their influence on the electromagnetic torque.

Superimposing a high-frequency square wave on the *d*-axis current permits the independent adjustment of its average value $i_{d\,av}$, and of its rms value $i_{d\,rms}$. Efficient braking at high dynamic performance and maximum system losses is then achieved in the following manner:

- The *q*-current controls the torque,
- the average *d*-current $i_{d\,av}$ controls the field, and
- the rms *d*-current $i_{d\,rms}$ controls the system losses.

The method is suited to maximize the system losses. It utilizes both the machine losses and the inverter losses to absorb the regenerated energy from the machine. Other than with dc braking, also the stator copper losses, the stator iron losses, and the inverter losses absorb braking energy. This increases the braking power significantly. The upper curve in Fig. 5 shows that the braking torque is much higher than with dc braking.

4.2 Control implementation

Fig. 7 shows the signal flow diagram of the braking control scheme. The system generates the stator current reference vector $\boldsymbol{i}_s^*$ for a standard implementation of field oriented current control. Being state of the art technology [1, 5], the details of this implementation including the PWM inverter and the induction motor are not shown in Fig. 7. They are contained in the shaded block in the upper right of Fig. 7. Standard output signals from this block represent the measured values of the dc link voltage u_d and mechanical angular velocity ω, and the estimated value of the rotor flux linkage Ψ_r, respectively. In a sensorless speed control system, ω can be replaced by its estimated value $\hat{\omega}$ without performance degradation.

Positive speed will be assumed throughout this discussion for simplicity. The torque is then positive in the motoring mode, and negative during regeneration and braking. If the motor runs at negative speed, the sign of the torque is negative in the motoring mode, and positive during regeneration and braking. Also the signs of the *q*-current, and of some particular control signals reverse when the speed reverses. Operation at negative speed will not be discussed since the pertaining operating conditions can be easily derived from the following discussion.

The four PI controllers in Fig. 7 serve the following purposes:

- The speed controller determines the *q*-current reference i_q^* which in turn controls the machine torque within the bounds set by limiter L2. The symmetrical limit values $\pm i_{q\lim}$ of limiter L2 are variable and determined by the signal $i_{q\lim}$ that is supplied by the voltage controller. All PI controllers in Fig. 4 with limited output signals have provision for anti-windup.
- The voltage controller is inactive during motoring operation. Its reference signal $u_{d\max}$ acts as a constant upper limit for the dc link voltage. The value $u_{d\max}$ is higher than any magnitude that the dc link voltage can ever assume while the diode front end rectifier is active. Therefore, $u_d < u_{d\max}$ holds at motoring. The output signal of the voltage controller tends to keep increasing, but gets bounded by limiter L1 to a maximum level $i_{q\max}$.

  In the braking mode, the machine regenerates the braking power through the inverter into the dc link. The voltage controller gets activated when the dc link voltage rises beyond its limit value $u_{d\max}$. The braking power is then controlled by the voltage controller which overrides the speed controller by limiting the braking torque.
- The flux controller generates the signal $i_{d\,av}$ which controls the average value of the *d*-current i_d.
- The loss controller serves to generate the signal $i_{d\,rms}$ which represents the required rms value of i_d^*. This signal is obtained as the output of limiter L4 and, as an rms value, can only assume positive values. Owing to the high dynamic performance of field oriented control, the signals $|\omega^*|$ and $|\omega|$ at the input of the loss controller in Fig. 7 are almost equal in the motoring mode. The signal $i_{d\,rms}$ is then very low and positive, or assumes zero value, since negative values are suppressed by the limiter L4. A signal level $i_{d\,rms} \approx 0$ indicates that the operating conditions require no additional losses be created in the machine.

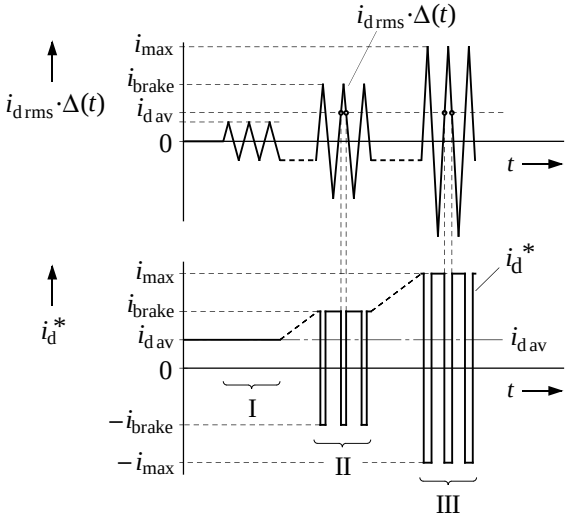

Fig. 8: Waveforms illustrating the operation in different braking modes; note that the switched waveforms in mode II and III have the same average value $i_{d\,av}$

The situation is different at braking operation which shall be explained next.

4.3 Pulse width and amplitude modulator

Braking is initiated when $|\omega^*| < |\omega|$. The output of the speed controller determines the *q*-current reference i_q^*, which turns negative at positive speed to control the braking torque. The regenerated braking power is absorbed by creating additional system losses. To this aim, the *d*-current reference i_d^* can assume two degrees of freedom: Its average value $i_{d\,av}$ controls the field, while its rms value $i_{d\,rms}$ controls the system losses. The composed signal $i_d^*(t)$ is generated as a switched waveform by a pulse width and pulse amplitude modulator.

The signal flow of this modulator is shown in the lower shaded block in Fig. 7. Its input signals are $i_{d\,av}$ and $i_{d\,rms}$, and the output signal is $i_d^*(t)$. The modulator is activated whenever $i_{d\,rms} > i_{d\,av}$, which level is referred to as i_{brake} in Fig. 8. The term indicates that braking power is dissipated by the system losses as commanded by the loss controller. Limiter L4 operates then in its linear range while $i_{d\,rms} < i_{max}$.

The modulator block comprises of an oscillator which generates a symmetrical triangular carrier wave $\Delta(t)$ of unity amplitude. The frequency of this carrier wave is set to

$$f_c > \frac{\omega_{sR}}{\tau_r}, \tag{8}$$

where τ_r is the normalized rotor time constant of the machine and ω_{sR} is the nominal stator frequency. The signal flow graph Fig. 6 illustrates that the rotor time constant characterizes a lowpass element between the switched waveform of $i_d(t)$ and the rotor flux. Condition (8) sets a lower limit for the carrier frequency which ensures that the harmonics contained in $i_d(t)$ do not produce undesired ripple in the rotor flux. There is no strict upper bound for f_c since the harmonic losses increase as the carrier frequency increases, which is beneficial, whereas the copper losses tend to gradually decrease. The reduction of the copper losses is only moderate but needs to be considered when choosing f_c. The reason is that $i_{d\,rms}$ reduces owing to the periodic transitions between i_{max} and $-i_{max}$, which exhibit a finite gradient. To summarize, the choice of f_c is not very critical. A coarse estimate of the rotor time constant is a good orientation which helps to satisfy condition (8). A typical value is f_c = 20 Hz for any medium power machine.

The unity carrier wave $\Delta(t)$ is adjusted by multiplier M2 to assume the magnitude $i_{d\,rms}$. The resulting signal $i_{d\,rms}\cdot\Delta(t)$ is compared with the modulator input signal $i_{d\,av}$ to generate a switching sequence in the comparator C1. The resulting duty cycle of the modulation is

$$d = \frac{1}{2}\left(1 + \frac{i_{d\,av}}{i_{d\,rms}}\right) \tag{9}$$

where $i_{d\,rms} > i_{d\,av}$.

The generated switching sequence has unity rms value since it oscillates between the signal levels +1 and –1. It is subsequently scaled in magnitude by multiplier M1 such that its rms value gets determined by the signal *a*.

Signal *a* is generated as follows: If $i_{\mathrm{drms}} > i_{\mathrm{dav}}$ as previously assumed, the limiter L3 receives a positive input signal and consequently outputs the value $i_{\mathrm{drms}} - i_{\mathrm{dav}}$ through its unity gain characteristic. To this value is the signal i_{dav} added, from which the signal $a = i_{\mathrm{drms}}$ results as the scaling factor for multiplier M1. The resulting reference signal $i_{\mathrm{d}}^*(t)$ is a pulsewidth modulated square wave of controllable amplitude. The signal is shown in the lower trace of Fig. 7 in time intervals II and III. The amplitude of this square wave and hence its rms value equals i_{drms}. The average value is given by

$$\bar{i}_{\mathrm{d}}^* = i_{\mathrm{drms}}(2d-1) \qquad (10)$$

Inserting the duty cycle from (9) into (10) yields $\bar{i}_{\mathrm{d}}^* = i_{\mathrm{dav}}$. Hence the switching sequence $i_{\mathrm{d}}^*(t)$ has the average value i_{dav} and the rms value i_{drms}. It forms the reference signal i_{d}^* for the underlying current control system.

The condition $i_{\mathrm{drms}} < i_{\mathrm{dav}}$ indicates that no additional system losses must be created. If $i_{\mathrm{drms}} < i_{\mathrm{dav}}$ is true, the output of limiter L3 is zero. The input of comparator C1 is $i_{\mathrm{dav}} - i_{\mathrm{drms}} \cdot \Delta(t)$ which is greater zero since $|\Delta(t)| \le 1$. Hence the output of comparator C1 is constant, and the modulator is deactivated.

4.4 Braking modes

Three different modes of operation can be defined at braking, depending on the speed and on the required braking power. The operating modes are explained with reference to the waveforms in Fig. 8.

Braking is initiated whenever the commanded speed ω^* is lower than the actual speed ω. The signal $|\omega^*| - |\omega|$ at the input of the loss controller in Fig. 7 turns negative, independently of the direction of rotation. Limiter L4 then enters its linear range. Its output signal i_{drms} assumes a positive value which indicates that loss control is activated. The level of i_{drms} controls the braking power and determines the braking mode.

4.4.1 Braking mode I

Time interval I in Fig. 8 illustrates the situation in braking mode I, in which the braking power is less than the regular system losses. A portion of the losses is then supplied from the dc link. The loss controller in Fig. 7 is active since $|\omega^*| - |\omega| < 0$. The generated signal i_{drms} is less than i_{dav}, which condition indicates that no additional losses need be generated. In fact, the condition has no significance since the rms value of a signal is at least greater than its average value.

In this situation, the amplitude of the output $i_{\mathrm{drms}} \cdot \Delta(t)$ of multiplier M2 is less than i_{dav} as shown in the upper trace of Fig. 8 for time interval I. The condition creates a constant unity signal at the output of comparator C1. Since $i_{\mathrm{drms}} < i_{\mathrm{dav}}$, the input to limiter L3 is negative and its output is zero. The signal *a* then assumes the value i_{dav}, which multiplies with the unity signal from C1 to form i_{d}^*. Hence the pulse and amplitude modulator is inactive. It creates the constant output signal $i_{\mathrm{d}}^* = i_{\mathrm{dav}}$.

4.4.2 Braking mode II

If the braking power exceeds the actual system losses, the rms current i_{drms} as generated from the loss controller increases beyond the value i_{dav} actually provided by the flux controller. The range $i_{\mathrm{dav}} < i_{\mathrm{drms}} < i_{\mathrm{max}}$ defines operation in braking mode II. The condition $i_{\mathrm{drms}} > i_{\mathrm{dav}}$ activates the pulse width and amplitude modulator as explained in the previous Section. The modulator generates a switching sequence $i_{\mathrm{d}}^*(t)$ having the average value i_{dav} and the rms value i_{drms}. This signal serves as the *d*-current reference. Its waveform is shown in the center portion of Fig. 8.

Three different current components are independently controlled in braking mode II: The average *d*-current i_{dav} is determined by the flux controller, the rms *d*-current i_{drms} is de-

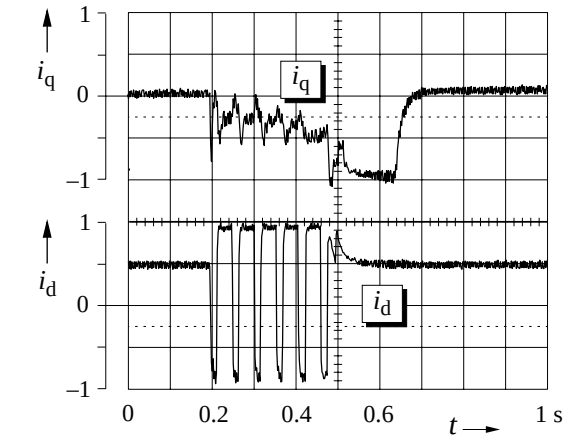

a) stator current components

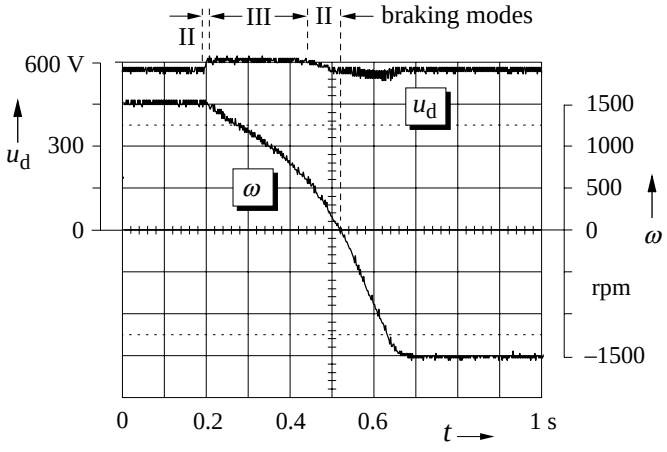

b) dc link voltage and speed

Fig. 9: Speed reversal with regenerative braking

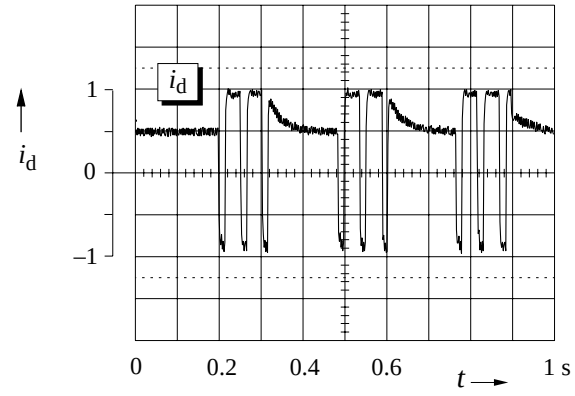

a) torque producing stator current component i_q

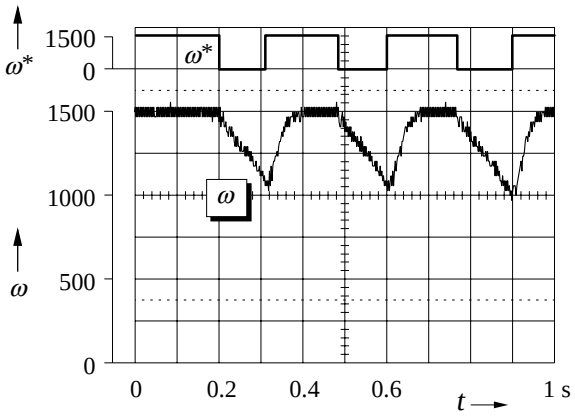

b) speed reference and actual speed

Fig. 10: Dynamic performance of the braking scheme, demonstrated by commanded high-frequency speed changes from nominal speed; the signal ω^* is not to scale.

termined by the loss controller, and the *q*-current i_q is governed by the speed controller.

In the base speed range, the machine is operated at nominal field. Operation above base speed requires field weakening to maintain the stator current controllable. The field is held at its highest possible value so as to maintain the stator core losses maximum. The copper losses in the stator and the rotor are adjusted by the loss controller such that the required braking power gets absorbed to the extent possible.

4.4.3 Braking mode III

Additional constraints exist when either the current limit of the inverter is reached, or the voltage limit of the dc link capacitor. Such conditions define braking mode III.

Current limiting may occur at low speed when a high braking torque is required. The braking power is then low and the dc voltage limit may not be reached. Current limiting during braking is done at the output of the loss controller. The purpose is served by limiter L4. Its upper bound i_{max} determines the amplitude of switching sequence $i_d^*(t)$ at the modulator output. The inverter currents are then also limited to about i_{max}, since the *q*-current does not contribute much to the rms stator current in braking mode III. It is small as compared with the maximum current i_{max}, and, moreover, it is in quadrature to the switched reference signal $i_d^*(t)$. Hence its contribution to the rms value of the stator currents is negligible.

Voltage limiting occurs above a certain speed level as the braking power is then higher. The regenerated braking power accumulates in the dc link capacitor which lets the dc link voltage rise. A higher dc link voltage favorably increases the switching losses of the inverter, which increases the permitted braking power.

If the required braking power exceeds the maximized system losses, the condition $u_d > u_{d\,max}$ activates the voltage controller in Fig. 7. The regenerated power must then reduce in order to limit the dc link voltage. The voltage controller reduces its output signal, and limiter L1 enters its linear range. Its reducing output signal $i_{q\,lim}$ narrows the bounds of the controllable limiter L2, thus reducing the magnitude of the negative *q*-current reference i_q^*. The torque producing current i_q^* is now controlled by the variable limit $i_{q\,lim}$, while the speed controller is deactivated. The voltage controller adjusts the braking torque through the signals $i_{q\,lim}$ and i_q^* such that $u_d \approx u_{d\,max}$ is maintained. The braking power is limited to the maximum permitted value.

The waveform of $i_d^*(t)$ in braking mode III is shown in Fig. 8, time interval III. Although the rms value is larger than that in braking mode II, the respective average values of $i_d^*(t)$ in braking modes II and III are adjusted to assume the same value $i_{d\,av}$, since $i_{d\,av}$ = const. in the base speed range. It can be observed in Fig. 8 that the duty cycle of switching sequence $i_d^*(t)$ changes accordingly.

It should be noted that braking at field oriented control can be either implemented as stator field orientation, or as rotor field orientation. It is of little significance which of the two alternatives apply in a particular application. It is important, though, that stator flux estimation in a sensorless control approach [5] remains stable even in the presence of residual high-frequency flux variations that originate from the pulsed waveforms of the *d*-axis current.

5. Experimental Results

The braking scheme was implemented in a 10-kW industrial PWM inverter drive. The control is based on stator field orientation without using a speed sensor. There were no hardware changes necessary; only the software was modified.

Fig. 9 shows a reversal of the speed from 1500 rpm to –1500 rpm. The machine starts immediately regenerating in braking mode II when the speed command is changed. The dc link voltage rises to over 600 V. The system losses are then increased by introducing high-frequency switching of the *d*-axis current i_d. The average value of i_d is maintained at nominal level to maintain the stator flux linkage at nominal value. Variations of the flux linkage are seen to be compensated by a periodic adjustment of the *q*-axis current. The higher spikes of i_q are due to imperfect dynamic decoupling from i_d, which

is a normal effect. Since the braking power is held constant by the voltage controller, torque pulsations do not occur.

The machine produces maximum braking torque and its speed reduces rapidly. The braking torque increases as the speed decreases which is seen from the average *q*-axis current and from the slope of the ω-curve. Braking mode II is enabled below 600 rpm. Below 500 rpm is the rms value of the *d*-axis current reduced: its originally regular and near rectangular waveform changes. Also the dc link voltage reduces.

Full negative torque is generated for acceleration in the reverse direction. Power is drawn from the dc link and the dc link voltage sags. It assumes its original higher value after reaching the steady-state.

Since braking takes about double the acceleration time in Fig. 9, the average braking torque is about half the maximum torque at motoring.

Fig. 10 illustrates the dynamic performance of the braking scheme in a sequence of high-frequency speed changes commanded from nominal speed.

6. SUMMARY

A novel control algorithm for induction motor drives enables regenerative braking without requiring power electronics hardware in addition to the regular diode rectifier front end. Such hardware was needed until now to dissipate accumulated braking power from the dc link, or to regenerate it into the feeding utility. Instead, the braking power is absorbed in the drive motor and in the inverter.

The braking control scheme maximizes the system losses. A loss controller is provided for this purpose. It serves for an independent adjustment of three different current components: the average value and the rms value of the *d*-axis current, and the *q*-axis current.

The algorithm is based on field oriented drive control and maintains the excellent dynamic performance also at braking. It is applicable to speed control systems with speed sensor and without speed sensor.

7. APPENDIX

The limiters in Fig. 7 have the following characteristics:

Limiter L1:

$$y = f(x) = \begin{cases} 0 & \text{for } x < 0 \\ x & \text{for } 0 \le x < i_{\mathrm{q\,max}} \\ i_{\mathrm{q\,max}} & \text{for } x \ge i_{\mathrm{q\,max}} \end{cases} \quad \text{(A1)}$$

Limiter L2:

$$y = f(x) = \begin{cases} -i_{\mathrm{q\,lim}} & \text{for } x < -i_{\mathrm{q\,lim}} \\ x & \text{for } -i_{\mathrm{q\,lim}} \le x < i_{\mathrm{q\,lim}} \\ i_{\mathrm{q\,lim}} & \text{for } x \ge i_{\mathrm{q\,lim}} \end{cases} \quad \text{(A2)}$$

Limiter L3:

$$y = f(x) = \begin{cases} 0 & \text{for } x \le 0 \\ x & \text{for } x > 0 \end{cases} \quad \text{(A3)}$$

Limiter L4:

$$y = f(x) = \begin{cases} i_{\max} & \text{for } x \le -i_{\max} \\ -x & \text{for } -i_{\max} < x \le 0 \\ 0 & \text{for } x > 0 \end{cases} \quad \text{(A4)}$$

8. REFERENCES

1. R. D. Lorenz, T. A. Lipo and D. W. Novotny, “Motion Control with Induction Motors”, in B. K. Bose (Editor) “Power Electronics and Variable Speed Drives”. *IEEE Press Book*, 1997.
2. S. Stadtfeld, “Braking Methods for Inverter Fed Induction Motors” (in German), *Antriebstechnik*, Vol. 32 (1993), No. 7, pp. 26-31.
3. J. Holtz: The Representation of AC Machine Dynamics by Complex Signal Flow Graphs. *IEEE Transactions on Industrial Electronics*, Vol. 42, No. 3 (1995), pp. 263-271.
4. Method of Braking a Vector Controlled Induction Machine, Control Device for Carying out this Method and Storage Medium. US and European Patents.
5. J. Holtz: Methods for Speed Sensorless Control of AC Drives, in K. Rajashekara (Editor) "Sensorless Control of AC Motors", *IEEE Press Book*, 1996.